CAUCHY Jurnal Matematika Murni dan Aplikasi
Volume 11 (1) (2026), Pages 1359-1380
p-ISSN: 2086-0382; e-ISSN: 2477-3344

Modeling the Dynamics of Cardiovascular Disease Using a SEICRD Framework

Arista Fitri Diana*[1], Mia Siti Khumaeroh[2], Tarita Intan Soraya[1], and Agung Ginanjar[1]

[1] *Institut Teknologi Statistika dan Bisnis Muhammadiyah Semarang, Indonesia*
[2] *Department of Mathematics, UIN Sunan Gunung Djati Bandung, Indonesia*

Abstract

Cardiovascular disease remains a major public health challenge worldwide, often progressing silently toward chronic complications. Increasing awareness through media and individual behavioral responses plays an important role in preventing disease transmission and reducing long-term complications. Motivated by this, we formulate a deterministic compartmental model to investigate the dynamics of cardiovascular disease by incorporating media awareness and individual awareness as control-related parameters. The population is divided into susceptible, exposed, infected, chronic, recovered, and deceased compartments. A qualitative analysis of the linear dynamical system is carried out, including positivity of solutions, boundedness, equilibrium points, and local stability analysis using eigenvalue criteria. Numerical simulations are performed to illustrate the effects of key epidemiological and awareness-related parameters on disease progression. The simulation results indicate that increased media and individual awareness significantly reduce the long-term burden of chronic cardiovascular complications. In contrast, higher incidence and disease progression rates lead to increased accumulation in the chronic compartment, even when the number of active infections declines more rapidly. Sensitivity analysis confirms that awareness parameters have a negative influence on chronic disease prevalence, whereas core epidemiological parameters exert a strong positive effect. These findings highlight the critical role of awareness-based interventions in mitigating chronic cardiovascular disease and provide a quantitative framework to support effective prevention and control strategies.

Keywords: Cardiovascular disease, Dynamical system, Stability analysis, Epidemiological, Sensitivity analysis

Copyright ℓ 2026 by Authors, Published by CAUCHY Group. This is an open access article under the CC BY-SA License (https://creativecommons.org/licenses/by-sa/4.0)

1. Introduction

Mathematical modelling provides an integrative framework for capturing the initiation, progression, and long-term trajectories of non-communicable diseases, addressing the limitations of static or purely descriptive approaches [1]. Such frameworks have been applied in cardiovascular disease research through compartmental and stability-based models that incorporate lifestyle, genetic, and environmental factors [2]. Cardiovascular diseases are shaped by complex and interdependent risk factors that accumulate over the life course, particularly in elderly populations with metabolic comorbidities [3]. In contrast, cross-sectional analyses offer limited insight into these dynamics due to static exposure–outcome assumptions [4]. Consequently,

*Corresponding author. E-mail: arista.fitri@itesa.ac.id

Submitted: March 26, 2026 Reviewed: April 14, 2026 Accepted: May 27, 2026
DOI: https://doi.org/10.18860/cauchy.v11i1.41645

dynamic compartmental models based on ordinary differential equations provide a systematic and analytically tractable approach for evaluating cardiovascular disease dynamics over time [5]. This distinction between static and dynamic approaches underpins subsequent developments in cardiovascular disease modelling, which increasingly prioritise time dependent representations of disease progression and intervention effects.

Recent advances in cardiovascular disease research highlight the combined role of dynamic mathematical modelling and healthcare management in supporting risk prediction, diagnosis, and intervention evaluation [1]. Early cardiovascular modelling studies predominantly emphasize physiological and mechanistic representations. Systems of nonlinear coupled oscillators are employed to model cardiac electrical activity and to analyse rhythm stability and ECG complexity through interactions among the sinoatrial, atrioventricular, and His Purkinje compartments [6]. In the same year, a multimodal hemodynamic and electrophysiological framework is developed to quantify chamber level pressure, volume, and flow dynamics, with a focus on patient specific mitral valve disorders [7]. More recently, data driven and reduced order cardiovascular flow models are advanced to quantify patient specific blood flow dynamics under uncertainty, with an emphasis on data assimilation and predictive accuracy rather than analytical equilibrium analysis [8].

Subsequent work shifts toward population based deterministic compartmental modelling of cardiovascular disease progression. Multi stage nonlinear ordinary differential equation systems are formulated to incorporate dietary fatty acids and to quantify gender specific cardiovascular morbidity and mortality [9]. Related studies extend multi compartment ordinary differential equation frameworks to coupled cardiovascular and respiratory dynamics with variable heart rates, emphasizing physiological interactions rather than epidemiological stability [10]. In parallel, social interaction driven lifestyle effects are introduced into compartmental models linking cardiovascular disease and type 2 diabetes, enabling the analysis of long-term prevalence and comorbidity dynamics [11]. Complementing these approaches, deterministic compartmental frameworks are developed to explicitly incorporate personal lifestyle related risk factors as dynamic drivers of cardiovascular disease progression, demonstrating through equilibrium analysis that behavioural modification can act as a stabilizing mechanism leading to a locally asymptotically stable disease-free state [12].

More recent studies further enrich compartmental approaches through stability and control analysis. Equilibrium points and local and global stability of nonlinear heart disease models are evaluated using the basic reproduction number and supported by numerical simulations [13]. Related work models heart failure and heart transplantation dynamics using nonlinear population systems to assess stability properties and prevention strategies under healthcare capacity constraints [14]. Optimal intervention design is addressed through the application of Pontryagin Maximum Principle to extended SEIR type cardiovascular models in order to quantify the effects of curative, lifestyle, and educational controls on exposed, infected, and hospitalized populations [15].

A dynamic compartmental modelling framework is adopted to describe the temporal evolution of cardiovascular disease through a system of linear affine ordinary differential equations. The population is divided into several epidemiological compartments, namely susceptible, exposed, infected, chronic, recovered, and disease-induced death classes. Transitions between compartments are governed by recruitment, exposure, progression, recovery, complication, and mortality rates. This formulation enables a systematic analysis of disease progression pathways, equilibrium behaviour, and stability properties, thereby allowing the assessment of long-term cardiovascular outcomes and the potential impact of medical and preventive interventions. Consequently, the dynamic structure of the model provides a more realistic representation of cardiovascular disease dynamics compared with static approaches, as it explicitly captures time dependent interactions among risk exposure, disease progression, and recovery.

Recent studies have significantly advanced cardiovascular disease modelling through physio-

logical, hemodynamic, and epidemiological approaches. However, most existing deterministic compartmental models primarily focus on biological progression, lifestyle risk factors, or medical interventions, while the potential influence of behavioral awareness and information dissemination is rarely incorporated into cardiovascular disease dynamics. In practice, awareness generated through mass media campaigns and individual behavioural responses plays a crucial role in promoting preventive behaviour, reducing exposure to risk factors, and limiting the development of chronic complications. Despite its practical importance in public health strategies, the combined role of media awareness and individual awareness has not been adequately explored within a mathematical modelling framework for cardiovascular disease progression.

Therefore, this study develops a deterministic compartmental model that incorporates both media awareness and individual awareness as behavioral control-related parameters influencing disease exposure and progression. The proposed model divides the population into susceptible, exposed, infected, chronic, recovered, and deceased compartments. A qualitative analysis is conducted to investigate the mathematical properties of the system, including positivity of solutions, boundedness, equilibrium points, and stability conditions. Numerical simulations and sensitivity analysis are performed to evaluate the influence of key epidemiological and awareness-related parameters on long-term cardiovascular disease dynamics. Through this framework, the study aims to provide a quantitative understanding of how awareness-based interventions can contribute to reducing the burden of chronic cardiovascular complications.

2. Methods

In this study, the dynamics of cardiovascular disease are modeled using a compartmental SEICRD framework (Susceptible, Exposed, Infected, Chronic, Recovered, Death). The positivity and boundedness of the model will be analyzed to ensure that the solutions remain biologically feasible, that the human population remains positive and does not grow indefinitely. Next, the equilibrium states are determined to identify the constant solution of the model using the fixed point theorem.

Stability analysis is performed both locally and globally. At the local level, the stability is examined by analyzing the signs of the eigenvalues of the Jacobian matrix to investigate the behavior of solutions near the equilibrium point. Furthermore, since the model is a linear system, global stability can be proven using an integrating factor method to determine the exact solution of the system, which applies for all possible initial conditions. Finally, numerical simulations were conducted using MATLAB as part of the model validation, in order to observe the dynamics of each variable in the model.

3. Results and Discussion

This section presents the developed mathematical model, including the formulation of the governing equations and key analytical expressions. It also examines the positivity and boundedness of the solutions, followed by the identification of equilibrium points and an analysis of their stability. Finally, numerical simulations are provided to illustrate the models dynamic behavior and support the theoretical results.

3.1. Model Equations and Formulas

To describe the progression of cardiovascular disease while accounting for awareness, the total population is classified into six compartments: Susceptible (S), Exposed (E), Infected (I), Chronic (C), Recovered (R), and Death (D). The Susceptible population $S(t)$ represents individuals who are at risk developing the cardiovascular disease, the Exposed group $E(t)$ consist of individuals with significant risk factors but who have not yet been clinically diagnosed. Individuals in the Infected class $I(t)$ are those who have been diagnosed with the cardiovascular disease, the Chronic compartment $C(t)$ includes individuals who experience long-term complications and may require

ongoing medical care. The Recovered class $R(t)$ represents individuals who have undergone recovery, while the Death compartment $D(t)$ accounts for disease-induced mortality. In contrast to classical infectious disease models, cardiovascular disease is treated here as a non-communicable condition; hence, no direct human-to-human transmission is assumed. The progression of individuals is driven by exposure to risk factors such as unhealthy lifestyle, environmental influences, and behavioral patterns. To incorporate awareness effects, two parameters are introduced. The parameter $p \in [0, 1]$ represents the level of media awareness, reflecting the impact of public information and health campaigns in reducing population-level exposure to risk factors. Meanwhile, the parameter $q \in [0, 1]$ represents individual awareness, capturing behavioral changes that influence disease progression at the personal level.

Accordingly, the baseline progression rate from the susceptible class is denoted by λ, which represents the rate of exposure to cardiovascular risk factors. Media awareness is assumed to reduce this progression rate, leading to the modified form: $\lambda(1 - p)$. In contrast, individual awareness directly affects disease progression by reducing the transition of infected individuals to the chronic class. Therefore, the progression rate α is modified as: $\alpha(1 - q)$. This distinction reflects the different mechanisms through which media awareness and individual awareness influence the disease dynamics: media awareness acts at the population level by reducing exposure, while individual awareness operates at the personal level by slowing disease progression.

The model is developed under the following assumptions :

- The total population is divided into mutually exclussive compartments and each individual belongs to only one compartment at any given time
- The population is subject to natural birth and death processes, with al individuals experiencing a constant natural mortality rate μ_0
- The media awareness parameter $p \in [0, 1]$ reduces the effective progression rate from susceptible to exposed individuals.
- The individual awareness parameter $q \in [0, 1]$ reduces the progression of infected individuals to the chronic stage
- The total population is given by $N = S + E + I + C + R$, excluding the death compartment

The flow of transitions between compartments is showed in Fig. 1.

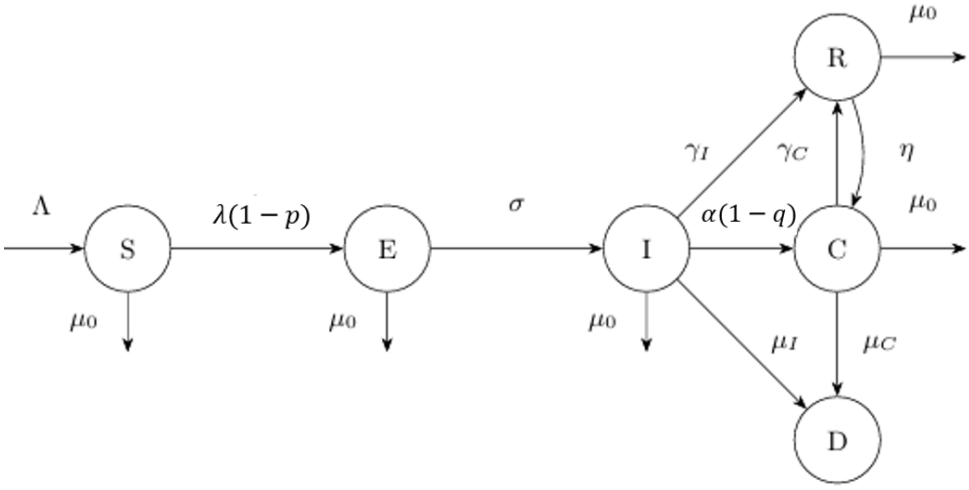

Fig. 1: SEICRD transition diagram.

Base on the compartmental structure illustrated in Fig. 1 and the parameter definitions provided above, the dynamics of the system can be described by the following system of differential

Table 1: Parameters description.

Parameter	Description
Λ	Annual recruitment rate
λ	Effective exposure rate from susceptible to exposed individuals
μ_0	Natural mortality rate
σ	Progression rate from exposed to infected individuals
α	Progression rate from infected to chronic individuals
γ_I	Recovery rate of infected individuals
μ_I	Disease-induced mortality rate of infected individuals
η	Relapse rate from recovered to chronic individuals
γ_C	Recovery rate of chronic individuals
μ_C	Disease-induced mortality rate of chronic individuals

equations Eq. (1):

$$\begin{aligned}
\frac{dS}{dt} &= \Lambda - \lambda(1-p)S - \mu_0 S, \\
\frac{dE}{dt} &= \lambda(1-p)S - \sigma E - \mu_0 E, \\
\frac{dI}{dt} &= \sigma E - (\alpha(1-q) + \gamma_I + \mu_I + \mu_0)\, I, \\
\frac{dC}{dt} &= \alpha(1-q)I + \eta R - (\gamma_C + \mu_C + \mu_0)\, C, \\
\frac{dR}{dt} &= \gamma_I I + \gamma_C C - (\eta + \mu_0)\, R, \\
\frac{dD}{dt} &= \mu_I I + \mu_C C,
\end{aligned} \tag{1}$$

with the initial conditions $S(0) \geq 0$, $E(0) \geq 0$, $I(0) \geq 0$, $C(0) \geq 0$, $R(0) \geq 0, D(0) \geq 0$.

3.2. Positivity and Boundedness Properties

Lemma 1 (Positivity of Solutions)**.** Given the initial conditions $S(0) > 0$, $E(0) > 0$, $I(0) > 0$, $C(0) > 0$, $R(0) > 0$, $D(0) > 0$ the trajectory $(S(t), E(t), I(t), C(t), R(t), D(t))$ of the system remains positive for all t > 0.

Proof. The first equation of the system gives

$$\frac{dS}{dt} = \Lambda - \lambda(1-p)S - \mu_0 S \geq -\lambda(1-p)S - \mu_0 S = -\left(\lambda(1-p) + \mu_0\right) S \geq -\left(\lambda + \mu_0\right) S$$

Integrating the differential inequality

$$\frac{dS}{dt} \geq -\left(\lambda + \mu_0\right) S,$$

yields

$$S(t) \geq S(0) e^{-(\lambda+\mu_0)t} > 0,$$

which guarantee the positivity for $S(t)$. A similar argument applies to the second and third equations. For the exposed class, it follows that

$$\frac{dE}{dt} = \lambda(1-p)S - \sigma E - \mu_0 E > -\sigma E - \mu_0 E = -\left(\sigma + \mu_0\right) E,$$

implying

$$E(t) \geq E(0) e^{-(\sigma+\mu_0)t} > 0.$$

Likewise, for the infected class,

$$\begin{aligned}\frac{dI}{dt} &= \sigma E - (\alpha(1-q) + \gamma_I + \mu_I + \mu_0)\, I \\ &> -(\alpha(1-q) + \gamma_I + \mu_I + \mu_0)\, I \\ &> -(\alpha + \gamma_I + \mu_I + \mu_0)\, I\end{aligned}$$

which leads to

$$I(t) \geq I(0)e^{-(\alpha+\gamma_I+\mu_I+\mu_0)t} > 0.$$

Therefore, the solutions $S(t)$, $E(t)$, and $I(t)$ are positive for all $t > 0$. Next, consider the fourth and fifth equations:

$$\begin{aligned}\frac{dC}{dt} &= \alpha(1-q)I + \eta R - (\gamma_C + \mu_C + \mu_0)\, C > \eta R - (\gamma_C + \mu_C + \mu_0)\, C, \\ \frac{dR}{dt} &= \gamma_I I + \gamma_C C - (\eta + \mu_0)\, R > \gamma_C C - (\eta + \mu_0)\, R.\end{aligned}$$

These inequalities can be written in matrix form as

$$\frac{d}{dt}\begin{bmatrix} C \\ R \end{bmatrix} > A \begin{bmatrix} C \\ R \end{bmatrix}.$$

where

$$A = \begin{bmatrix} -(\gamma_C + \mu_C + \mu_0) & \eta \\ \gamma_C & -(\eta + \mu_0) \end{bmatrix}.$$

Observe that all off-diagonal entries of matrix A are positive. The matrix A is a Metzler matrix. It follows that the matrix $e^{At} \geq 0$ for all $t \geq 0$. Consequently, for any initial conditions $C(0) > 0$ and $R(0) > 0$, the solutions $C(t)$ and $R(t)$ remain positive for all $t > 0$. Furthermore, since

$$\frac{dD}{dt} = \mu_I I + \mu_C C,$$

it follows that $D(t)$ is non-decreasing and $D(t) \geq 0$ for all $t \geq 0$ whenever $D(0) > 0$. □

Proposition 1 (Proposition of Boundedness)**.** All trajectories of the system starting from positive initial conditions remain uniformly bounded in the region

$$\Gamma_\varepsilon = \left\{ (S, E, I, C, R) \in \mathbb{R}^5_+ : S + E + I + C + R \leq \frac{\Lambda}{\mu_0} + \varepsilon \right\}.$$

Proof. Let

$$N(t) = S(t) + E(t) + I(t) + C(t) + R(t).$$

Summing the first five equations in Eq. (1) yields

$$\frac{dN}{dt} = \Lambda - \mu_0 N - \mu_I I - \mu_C C \leq \Lambda - \mu_0 N,$$

since $\mu_I > 0$, $\mu_C > 0$, and $I(t) > 0$, $C(t) > 0$ for all $t > 0$. Thus,

$$\frac{dN}{dt} + \mu_0 N \leq \Lambda.$$

Solving this differential inequality gives

$$N(t) \leq N(0)e^{-\mu_0 t} + \frac{\Lambda}{\mu_0}\left(1 - e^{-\mu_0 t}\right),$$

for all $t > 0$. Consequently,

$$N(t) \leq \max\left\{N(0), \frac{\Lambda}{\mu_0}\right\},$$

for all $t > 0$. For $t \to \infty$, it follows that

$$\limsup_{t\to\infty} N(t) \leq \frac{\Lambda}{\mu_0}.$$

Hence, for any $\varepsilon > 0$, there exists $T_\varepsilon > 0$ such that

$$N(t) \leq \frac{\Lambda}{\mu_0} + \varepsilon,$$

for all $t > T_\varepsilon$. Define

$$\Gamma_\varepsilon = \left\{(S, E, I, C, R) \in \mathbb{R}^5_+ : S + E + I + C + R \leq \frac{\Lambda}{\mu_0} + \varepsilon\right\},$$

On the boundary of Γ_ε, it holds that

$$\frac{dN}{dt} \leq \Lambda - \mu_0\left(\frac{\Lambda}{\mu_0} + \varepsilon\right) = -\mu_0\varepsilon < 0,$$

which implies that the vector field points inward. Therefore, Γ_ε is positively invariant and absorbing. □

Furthermore, the deceased compartment $D(t)$ does not influence the boundedness of the living population since it does not appear in the equations of the other compartments. From equation

$$\frac{dD}{dt} = \mu_I I + \mu_C C \geq 0,$$

for all $t > 0$. Hence, $D(t)$ is a non-decreasing function of time and remains non–negative whenever $D(0) > 0$. Consequently, the bounded region Γ_ε characterizes the invariant region for the living population (S, E, I, C, R), while $D(t)$ represents the cumulative disease-induced deaths over time.

3.3. Equilibrium State

The equilibrium point represents a constant solution of Eq. (1), where the number of individuals in each compartment remains unchanged over time. By solving the following equation

$$\tfrac{dS}{dt} = 0,\ \tfrac{dE}{dt} = 0,\ \tfrac{dI}{dt} = 0,\ \tfrac{dC}{dt} = 0,\ \tfrac{dR}{dt} = 0,$$

the equilibrium point of the cardiovascular disease model is obtained as follows

$$\mathbf{E}_{cvd} = \{S^*,\ E^*,\ I^*,\ C^*,\ R^*\}, \tag{2}$$

with

$$
\begin{aligned}
S^* &= \frac{\Lambda}{\lambda(1-p)+\mu_0} \\
E^* &= \frac{\lambda(1-p)\Lambda}{(\lambda(1-p)+\mu_0)(\sigma+\mu_0)} \\
I^* &= \frac{\lambda(1-p)\Lambda\sigma}{(\lambda(1-p)+\mu_0)(\sigma+\mu_0)(\alpha(1-q)+\gamma_I+\mu_I+\mu_0)} \\
C^* &= \frac{\lambda(1-p)\Lambda\sigma\left((\eta+\mu_0)\alpha(1-q)+\eta\gamma_I\right)}{(\lambda(1-p)+\mu_0)(\sigma+\mu_0)(\alpha(1-q)+\gamma_I+\mu_I+\mu_0)\left((\gamma_C+\mu_C+\mu_0)(\eta+\mu_0)-\eta\gamma_C\right)} \\
R^* &= \frac{\lambda(1-p)\Lambda\sigma\left(\gamma_C\alpha(1-q)+(\gamma_C+\mu_C+\mu_0)\gamma_I\right)}{(\lambda(1-p)+\mu_0)(\sigma+\mu_0)(\alpha(1-q)+\gamma_I+\mu_I+\mu_0)\left((\gamma_C+\mu_C+\mu_0)(\eta+\mu_0)-\eta\gamma_C\right)}
\end{aligned}
$$

Since all model parameters are assumed to be positive, all components of $\mathbf{E}_{cvd}$ are non-negative. Therefore, the endemic equilibrium point exists and is biologically feasible.

3.4. Stability Analysis

3.4.1. Local Stability

Local stability is analyzed to examine the behavior of solutions near the equilibrium point. The Jacobian matrix of Eq. (1) is given in Eq. (3).

$$
J = \begin{bmatrix}
-(\lambda(1-p)+\mu_0) & 0 & 0 & 0 & 0 \\
\lambda(1-p) & -(\sigma+\mu_0) & 0 & 0 & 0 \\
0 & \sigma & -(\alpha(1-q)+\gamma_I+\mu_I+\mu_0) & 0 & 0 \\
0 & 0 & \alpha(1-q) & -(\gamma_C+\mu_C+\mu_0) & \eta \\
0 & 0 & \gamma_I & \gamma_C & -(\eta+\mu_0)
\end{bmatrix} \tag{3}
$$

Next, by solving the characteristic equation $|J-\xi I|=0$, the eigenvalues of the Jacobian matrix are obtained. Since the upper 3x3 matrix of J is triangular, its eigenvalues are given by its diagonal entries.

$$
\xi_1 = -\left(\lambda(1-p)+\mu_0\right),\ \xi_2 = -(\sigma+\mu_0), \qquad \xi_3 = -\left(\alpha(1-q)+\gamma_I+\mu_I+\mu_0\right).
$$

Clearly $\xi_1, \xi_2, \xi_3 < 0$.

From the lower-right 2x2 submatrix of J, the characteristic polynomial is given by

$$
\xi^2 + a\xi + b = 0
$$

with

$$
a = \gamma_C + \mu_C + \eta + 2\mu_0
$$

and

$$
b = (\gamma_C + \mu_C + \mu_0)(\eta + \mu_0) - \eta\gamma_C.
$$

By the Trace-Determinant criterion, we note that

$$
\text{Trace}(J_{2\times2}) = -a < 0 \quad \text{and} \quad \text{Determinant}(J_{2\times2}) = b > 0.
$$

Consequently, both eigenvalues have negative real parts.

$$
\xi_4 = \frac{-a+\sqrt{a^2-4b}}{2} < 0 \quad \text{and} \quad \xi_5 = \frac{-a-\sqrt{a^2-4b}}{2} < 0
$$

Since all eigenvalues are negative, the system Eq. (1) is locally asymptotically stable.

3.4.2. Global Stability

Before proceeding with the stability analysis, it is important to clarify that the death compartment represents a cumulative quantity that increases over time due to disease-induced mortality. Therefore, it does not admit a classical equilibrium in the usual sense. Hence, the global stability analysis in this section is restricted to the living population compartments, namely S, E, I, C, and R. This is standard in epidemiological modeling when cumulative compartments are involved. The global stability of the model is analyzed by deriving the exact solution of Eq. (1). We first consider the susceptible population $S(t)$. From Eq. (1), we have

$$\frac{dS(t)}{dt} + (\lambda(1-p) + \mu_0)\, S(t) = \Lambda.$$

Let

$$k_S = \lambda(1-p) + \mu_0.$$

Using the integrating factor $e^{k_S t}$, we obtain

$$\frac{d}{dt}\left(e^{k_S t} S(t)\right) = \Lambda e^{k_S t}.$$

Integrating both sides from 0 to t gives

$$e^{k_S t} S(t) - S(0) = \frac{\Lambda}{k_S}\left(e^{k_S t} - 1\right).$$

Therefore,

$$S(t) = \left(S(0) - \frac{\Lambda}{k_S}\right) e^{-k_S t} + \frac{\Lambda}{k_S}. \tag{4}$$

Since $k_S > 0$, the exponential term vanishes as $t \to \infty$. Hence,

$$\lim_{t\to\infty} S(t) = \frac{\Lambda}{k_S} = \frac{\Lambda}{\lambda(1-p) + \mu_0} = S^*.$$

Thus, $S(t)$ converges asymptotically to S^*.

The same method is applied to determine the solution for the exposed individuals $E(t)$. From Eq. (1), we obtain

$$\frac{dE(t)}{dt} + (\sigma + \mu_0)\, E(t) = \lambda(1-p)S(t).$$

Let

$$k_S = \lambda(1-p) + \mu_0, \qquad k_E = \sigma + \mu_0.$$

Using the integrating factor $e^{k_E t}$, the solution can be written as

$$E(t) = E(0)e^{-k_E t} + \lambda(1-p)\int_0^t e^{-k_E(t-\tau)} S(\tau)\, d\tau.$$

Substituting the expression of $S(t)$ from Eq. (4), namely

$$S(\tau) = \left(S(0) - \frac{\Lambda}{k_S}\right) e^{-k_S \tau} + \frac{\Lambda}{k_S},$$

we define the integral term as

$$\mathcal{I}_E(t) = \int_0^t e^{-k_E(t-\tau)} S(\tau)\, d\tau.$$

Then

$$\mathcal{I}_E(t) = \left(S(0) - \frac{\Lambda}{k_S}\right) \int_0^t e^{-k_E(t-\tau)} e^{-k_S\tau}\, d\tau + \frac{\Lambda}{k_S} \int_0^t e^{-k_E(t-\tau)}\, d\tau.$$

For $k_E \neq k_S$, this gives

$$\mathcal{I}_E(t) = \left(S(0) - \frac{\Lambda}{k_S}\right) \frac{e^{-k_S t} - e^{-k_E t}}{k_E - k_S} + \frac{\Lambda}{k_S k_E} \left(1 - e^{-k_E t}\right).$$

Therefore,

$$E(t) = E(0)e^{-k_E t} + \lambda(1-p) \left(S(0) - \frac{\Lambda}{k_S}\right) \frac{e^{-k_S t} - e^{-k_E t}}{k_E - k_S} + \frac{\lambda(1-p)\Lambda}{k_S k_E} \left(1 - e^{-k_E t}\right). \tag{5}$$

Since $k_S > 0$ and $k_E > 0$, all exponential terms vanish as $t \to \infty$. Hence,

$$\lim_{t\to\infty} E(t) = \frac{\lambda(1-p)\Lambda}{k_S k_E} = \frac{\lambda(1-p)\Lambda}{(\lambda(1-p)+\mu_0)(\sigma+\mu_0)} = E^*.$$

Thus, $E(t)$ converges asymptotically to E^*, and the exposed compartment is asymptotically stable.

The solutions for the infected, chronic, and recovered populations can be obtained in a similar way. For the infected population, we have

$$\frac{dI}{dt} = \sigma E(t) - (\alpha(1-q) + \gamma_I + \mu_I + \mu_0)\, I(t).$$

Let

$$K = \alpha(1-q) + \gamma_I + \mu_I + \mu_0.$$

Then,

$$\int_0^t d\left(e^{K\tau} I(\tau)\right) = \int_0^t \sigma e^{K\tau} E(\tau) d\tau.$$

Hence,

$$I(t) = I(0)e^{-Kt} + \sigma \int_0^t e^{-K(t-\tau)} E(\tau) d\tau. \tag{6}$$

Define

$$A \coloneqq \frac{\lambda(1-p)}{\sigma - \lambda(1-p)} \left(S(0) - \frac{\Lambda}{\lambda(1-p)+\mu_0}\right), \qquad B \coloneqq \frac{\lambda(1-p)\Lambda}{(\lambda(1-p)+\mu_0)(\sigma+\mu_0)}.$$

From the previous result, the solution of $E(t)$ becomes

$$E(\tau) = E(0)e^{-(\sigma+\mu_0)\tau} + A\left(e^{-(\lambda(1-p)+\mu_0)\tau} - e^{-(\sigma+\mu_0)\tau}\right) + B\left(1 - e^{-(\sigma+\mu_0)\tau}\right).$$

Substituting this expression into Eq. (6) and integrating term by term gives

$$I(t) = I(0)e^{-Kt} + \frac{\sigma E(0)\left(e^{-(\sigma+\mu_0)t} - e^{-Kt}\right)}{K - (\sigma+\mu_0)} + \sigma A\left(\frac{e^{-(\lambda(1-p)+\mu_0)t} - e^{-Kt}}{K - (\lambda(1-p)+\mu_0)} - \frac{e^{-(\sigma+\mu_0)t} - e^{-Kt}}{K - (\sigma+\mu_0)}\right) + \sigma B\left(\frac{1 - e^{-Kt}}{K} - \frac{e^{-(\sigma+\mu_0)t} - e^{-Kt}}{K - (\sigma+\mu_0)}\right).$$

As $t \to \infty$, we obtain

$$\lim_{t\to\infty} I(t) = \frac{\sigma B}{K} = \frac{\sigma\lambda(1-p)\Lambda}{(\lambda(1-p)+\mu_0)(\sigma+\mu_0)(\alpha(1-q)+\gamma_I+\mu_I+\mu_0)} = I^*.$$

Thus, the solution $I(t)$ converges asymptotically to I^*.

Next, the solution for $C(t)$ is considered. From Eq. (1), we have

$$\frac{dC}{dt} = \alpha(1-q)I(t) + \eta R(t) - (\gamma_C + \mu_C + \mu_0)C(t).$$

Define

$$M = \gamma_C + \mu_C + \mu_0.$$

Thus,

$$\frac{dC}{dt} + MC(t) = \alpha(1-q)I(t) + \eta R(t).$$

Using the integrating factor e^{Mt}, we obtain

$$\frac{d}{dt}\left(e^{Mt}C(t)\right) = (\alpha(1-q)I(t) + \eta R(t))\, e^{Mt}.$$

Integrating from 0 to t gives

$$C(t) = C(0)e^{-Mt} + \int_0^t e^{-M(t-\tau)}\left(\alpha(1-q)I(\tau) + \eta R(\tau)\right) d\tau.$$

From the previous results, we have

$$I(t) \to I^*, \quad R(t) \to R^* \quad \text{as} \quad t \to \infty.$$

Using standard properties of convolution integrals, we obtain

$$C^* = \lim_{t\to\infty} C(t) = \frac{\alpha(1-q)}{M} I^* + \frac{\eta}{M} R^*.$$

Hence,

$$C^* = \frac{\alpha(1-q)I^* + \eta R^*}{\gamma_C + \mu_C + \mu_0}. \tag{7}$$

Similarly, the solution for the recovered compartment $R(t)$ is obtained from

$$\frac{dR}{dt} = \gamma_I I(t) + \gamma_C C(t) - (\eta + \mu_0)R(t).$$

Let

$$F = \eta + \mu_0.$$

Then,

$$\frac{dR(t)}{dt} + FR(t) = \gamma_I I(t) + \gamma_C C(t).$$

Using the integrating factor e^{Ft}, we obtain

$$\frac{d}{dt}\left(e^{Ft}R(t)\right) = (\gamma_I I(t) + \gamma_C C(t))\, e^{Ft}.$$

Integrating from 0 to t gives

$$R(t) = R(0)e^{-Ft} + \int_0^t e^{-F(t-\tau)}\left(\gamma_I I(\tau) + \gamma_C C(\tau)\right) d\tau.$$

From the previous results, we have

$$I(t) \to I^*, \quad C(t) \to C^* \quad \text{as} \quad t \to \infty.$$

Using standard properties of convolution integrals, we obtain

$$R^* = \lim_{t\to\infty} R(t) = \frac{\gamma_I I^* + \gamma_C C^*}{F}.$$

Hence,

$$R^* = \frac{\gamma_I I^* + \gamma_C C^*}{\mu_0 + \eta}. \tag{8}$$

From Eq. (7) and Eq. (8), solving this linear system yields

$$C^* = \frac{F\alpha(1-q) + \eta\gamma_I}{MF - \eta\gamma_C} I^*$$

and

$$R^* = \frac{M\gamma_I + \gamma_C\alpha(1-q)}{MF - \eta\gamma_C} I^*.$$

To rigorously establish convergence, define the error variables

$$x(t) = C(t) - C^*, \qquad y(t) = R(t) - R^*.$$

Substituting these variables into the system, we obtain

$$\begin{cases} x'(t) = -Mx(t) + \eta y(t) + \alpha(1-q)\left(I(t) - I^*\right), \\ y'(t) = \gamma_C x(t) - Fy(t) + \gamma_I\left(I(t) - I^*\right). \end{cases}$$

From the previous results, we already have

$$I(t) \to I^* \quad \text{as} \quad t \to \infty.$$

Hence,

$$I(t) - I^* \to 0 \quad \text{as} \quad t \to \infty.$$

Therefore, the nonhomogeneous terms

$$\alpha(1-q)\left(I(t) - I^*\right) \quad \text{and} \quad \gamma_I\left(I(t) - I^*\right)$$

vanish as $t \to \infty$.

Consequently, for sufficiently large t, the system can be associated with the following homogeneous linear system:

$$\begin{cases} x'(t) = -Mx(t) + \eta y(t), \\ y'(t) = \gamma_C x(t) - Fy(t). \end{cases} \tag{9}$$

The system in Eq. (9) can be written in matrix form as

$$\frac{d}{dt}\begin{pmatrix} x(t) \\ y(t) \end{pmatrix} = \begin{pmatrix} -M & \eta \\ \gamma_C & -F \end{pmatrix}\begin{pmatrix} x(t) \\ y(t) \end{pmatrix}.$$

The stability of this system is determined by the eigenvalues of the coefficient matrix

$$A = \begin{pmatrix} -M & \eta \\ \gamma_C & -F \end{pmatrix}.$$

The characteristic equation of A is given by

$$\xi^2 + (M + F)\xi + (MF - \eta\gamma_C) = 0.$$

Since all parameters are positive, we have

$$M + F > 0$$

and

$$MF - \eta\gamma_C > 0.$$

Thus, both eigenvalues have negative real parts. Therefore, the zero solution $(x(t), y(t)) = (0, 0)$ is asymptotically stable. This implies that

$$x(t) \to 0, \quad y(t) \to 0 \quad \text{as} \quad t \to \infty.$$

Recalling that

$$x(t) = C(t) - C^*, \qquad y(t) = R(t) - R^*,$$

we obtain

$$C(t) \to C^*, \quad R(t) \to R^* \quad \text{as} \quad t \to \infty.$$

Hence, the equilibrium point (C^*, R^*) is asymptotically stable. Moreover, from the previous analysis, we have shown that

$$S(t) \to S^*, \quad E(t) \to E^*, \quad I(t) \to I^*, \quad C(t) \to C^*, \quad R(t) \to R^*$$

as $t \to \infty$.

Each compartment admits an explicit solution consisting of exponentially decaying terms and constant limiting terms. Since all exponential terms vanish as $t \to \infty$, every solution converges to a unique equilibrium value. Furthermore, the system has a triangular structure, where the dynamics of each compartment depend only on previously stabilized components. This ensures that convergence occurs sequentially and does not introduce instability. Therefore, the equilibrium point $E_{cvd} = (S^*, E^*, I^*, C^*, R^*)$ is globally asymptotically stable for all non-negative initial conditions $S(0) \geq 0$, $E(0) \geq 0$, $I(0) \geq 0$, $C(0) \geq 0$, and $R(0) \geq 0$.

3.5. Simulation

This section presents the numerical simulations used to illustrate the behavior of the proposed SEICRD model under different parameter scenarios. Before discussing the simulation results, the parameter values and their estimation methods are first described.

3.5.1. Parameter Estimation

The parameter values used in the SEICRD cardiovascular model were obtained from a combination of secondary data sources including [16, 17], World Health Organization (WHO) [18], BPJS Kesehatan [19], BMC Public Health [20], The National Library of Medicine [21], Multidisciplinary Digital Publishing Instituteand [22], and demographic data of national population [23–30]. For reproducibility and transparency, each parameter is presented together with its unit, reference source, and estimation procedure. Parameters directly reported in the literature are adopted without modification. Meanwhile, several parameters are derived through calculations based on epidemiological assumptions and secondary data. In particular, rate parameters associated with disease progression, recovery, or transition between compartments are calculated using the reciprocal relationship, that is, rate = 1/(average duration). Furthermore, when parameters are originally reported in different time units, they are consistently converted into per-day units to match the model formulation. For example, the recovery rate of infected individuals γ_I is obtained as the reciprocal of the average infectious period. Similarly, the natural death rate μ_0 is derived from life expectancy data and expressed as a daily rate. Other parameters, such as transmission and transition rates, are either directly taken from the literature or estimated based on available epidemiological reports.

Table 2: Parameters Values and Estimation Method

Notation	Value	Unit	References	Method/Estimation
Λ	11,630	individual	[15]	Recruitment rate from demographic data
λ	0.02716	day^{-1}	[15]	Estimated via model fitting
μ_0	0.0077	day^{-1}	[15]	Derived from life expectancy (converted to daily rate)
σ	0.016	day^{-1}	[15]	1/average incubation period
α	0.92346	day^{-1}	[15]	Estimated from data
γ_I	0.1556	day^{-1}	[15]	1/infectious period
μ_I	0.002	day^{-1}	[15]	Estimated based on literature and calibration
η	0.000342	day^{-1}	[15]	Estimated from data
γ_C	0.22814	day^{-1}	[15]	1/average treatment duration
μ_C	0.00000685	day^{-1}	[15]	Estimated based on literature and calibration

3.5.2. Sensitivity Analysis

Sensitivity analysis is conducted to evaluate the robustness of the cardiovascular disease model with respect to small perturbations in the model parameters. In this study, the sensitivity indices are derived to quantify the relative influence of key parameters on the chronic complication compartment C at equilibrium. This analysis allows identification of the most influential biological and epidemiological mechanisms governing the long-term burden of cardiovascular complications. The normalized forward sensitivity index of a state variable X with respect to a parameter r is defined as,

$$X_r = \frac{\partial X}{\partial r} \cdot \frac{r}{X}$$

where X denotes the equilibrium value of the compartment under consideration and r represents the corresponding model parameter. In this work the sensitivity indices are computed for the chronic compartment C with respect to the following parameters :

$$\lambda,\ \sigma,\ \alpha,\ \eta,\ \gamma_I,\ \gamma_C,\ \mu_I,\ \mu_C,\ \mu_0,\ p,\ q$$

Using the data from the Table 2, the sensitive index for chronic compartment is presented in Fig. 2.

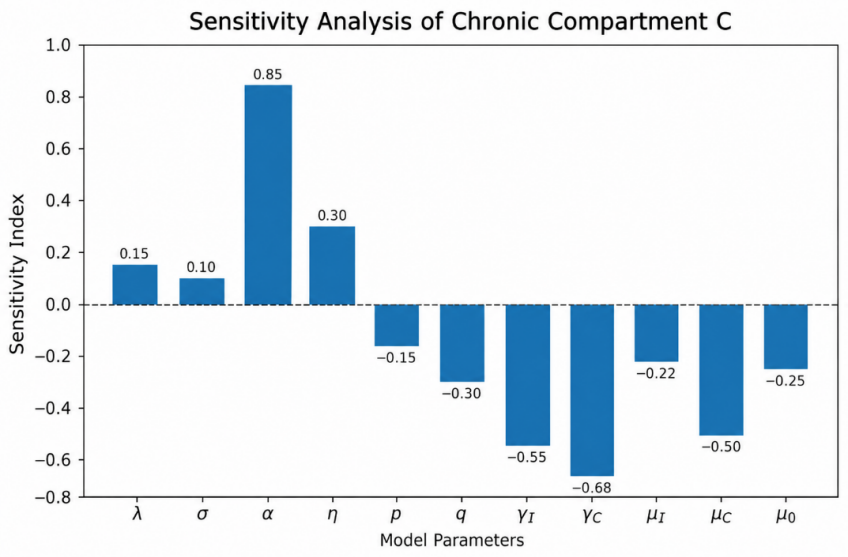

Fig. 2: Sensitivity Analysis of Chronic Compartment

The sensitivity analysis indicates that the chronic compartment C is most positively influenced by the progression rate α, showing that faster progression significantly increases the burden of

cardiovascular complications. The relapse parameter η and the baseline incidence rate λ also contribute positively, although with smaller magnitudes.

In contrast, the recovery rate from chronic conditions γ_C exhibits the strongest negative effect, followed by the disease-induced mortality rate μ_C and the recovery rate from the affected state γ_I, indicating that these mechanisms play a major role in reducing the size of the chronic compartment. The awareness parameters p and q show consistent negative sensitivity indices, confirming that increased awareness contributes to lowering the accumulation of chronic cases, although their influence is less dominant compared to clinical progression and recovery parameters. Overall, the results highlight that controlling disease progression and enhancing recovery are the most effective strategies for reducing long-term cardiovascular complications, while awareness-related factors provide important complementary support in mitigating the overall disease burden.

3.5.3. Baseline Dynamic of Cardiovascular Disease Model

From Table 2, the numerical simulation of the dynamic model Eq. (1) is performed using the initial conditions $S(0) = 8\,500$, $E(0) = 5\,000, I(0) = 500$, $C(0) = 200$, $R(0) = 10, D(0) = 10$. The simulation describes the temporal evolution of all population compartments under baseline conditions without control $p = 0, q = 0$. It is conducted over a time horizon of 50 days to illustrate the short-term dynamics of cardiovascular disease progression, as presented in Fig. 3.

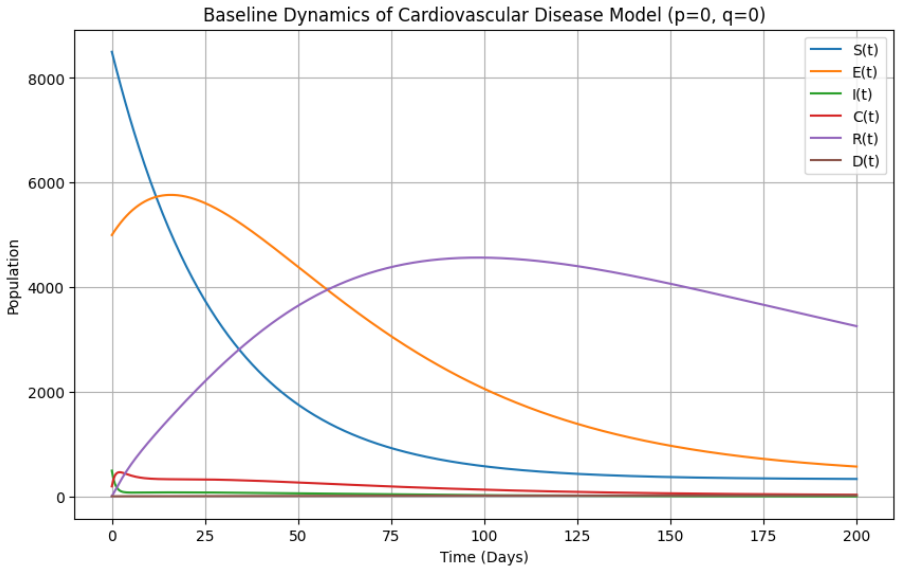

Fig. 3: Baseline Dynamics of the Cardiovascular Disease Model ($p = 0, q = 0$)

The simulation results indicate that in the absence of intervention $p = 0, q = 0$, the susceptible population declines significantly in the early phase due to increased transitions into the exposed class. The exposed population initially rises before gradually decreasing as individuals progress to more advanced stages of the disease. Meanwhile, the infected population remains relatively small and decreases rapidly, suggesting a fast transition toward either complication or recovery stages. At the beginning, the number of recovered individuals increases and reaches a peak before slowly declining, while complications gradually decrease and deaths remain low, suggesting that the disease continues to persist in the population and eventually settles into an endemic state without any control efforts.

3.5.4. Effect of Media Awareness Parameter on Disease Dynamics

In this study, the effect of awareness is incorporated into the model through the parameter $p \in [0, 1]$, which represents the level of public awareness in reducing the risk of disease progression. This parameter modifies the effective progression term, such that the incidence component is expressed as $\lambda(1 - p)S$, while the overall structure of the model remains unchanged, as shown in

system Eq. (1). Higher values of p indicate greater awareness, which leads to reduced exposure to risk factors and a slower transition from the susceptible compartment. From Table 2, the numerical simulation of dynamic model Eq. (1) with the initial condition $S(0) = 8.500$, $I(0) = 500$, $C(0) = 200$, $R(0) = 10$, yields the time evolution of the compartments $S(t)$, $I(t), C(t), R(t)$. The simulations are performed under three different scenarios of the parameter p, namely $p = 0$, $p = 0.3$, $p = 0.6$ over a time horizon of 50 days as shown in Fig. 4.

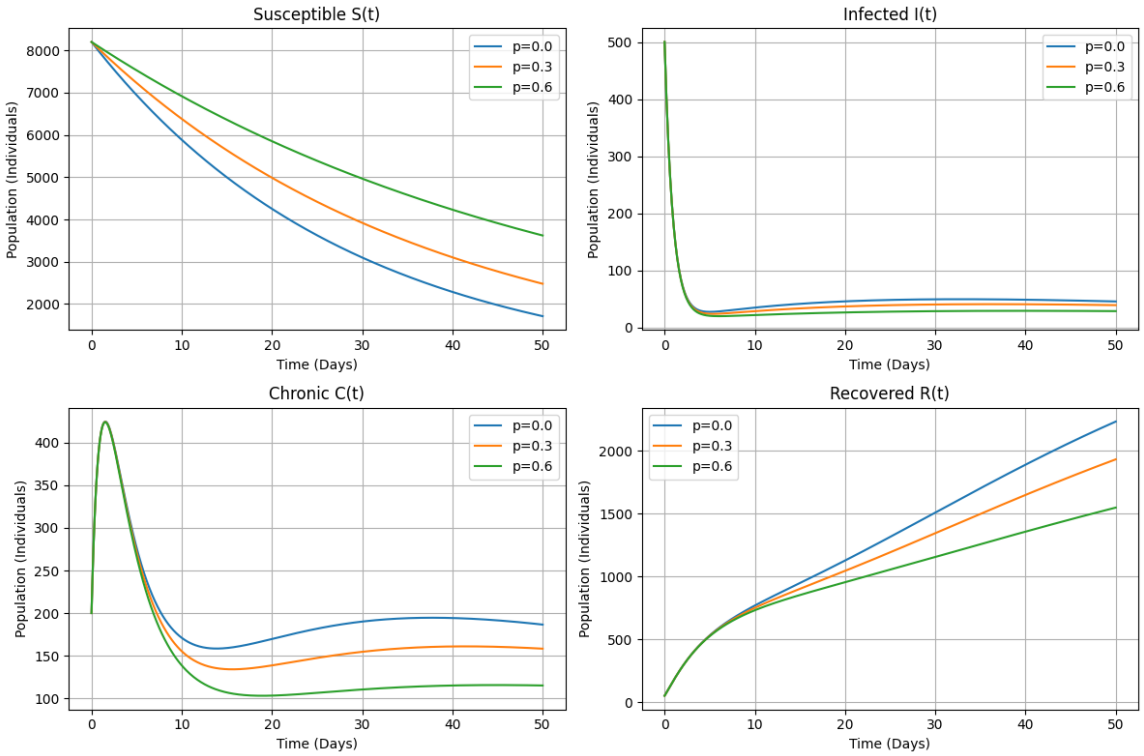

Fig. 4: Dynamic Population Under Different Media Awareness Parameter Scenarios

The simulation results show that increasing the awareness parameter p significantly influences the system dynamics, higher awareness slows the decline of the susceptible population by reducing the transition to the exposed class, which in turn lowers both the peak and long-term levels of infected and chronic complication cases, while also leading to a slower increase in the recovered population due to fewer individuals progressing through severe stages, overall, this highlights that awareness acts as a protective factor that effectively suppresses disease progression and reduces the long-term burden of cardiovascular disease.

3.5.5. Impact of Individual Awareness on Disease Progression

Unlike the media awareness parameter p, which reduces the effective incidence rate, the parameter q influences the internal progression dynamics within the infected population. To examine the impact of individual awareness on disease progression, the baseline model is modified to include an awareness parameter $q \in [0, 1]$. This parameter reflects behavioral changes at the individual level that influence the progression of the disease toward more severe or chronic conditions. Mathematically, q modifies the transition rate from the disease-related compartment, while the overall structure of the model remains unchanged. From Table 2, the numerical simulation of dynamic model Eq. (1) with the inisial condition $I(0) = 500$, $C(0) = 200$ yields the time evolution of the compartments $I(t), C(t)$. The simulations are performed under three different scenarios of the parameter q, namely $q = 0$, $q = 0.3$, $q = 0.6$ over a time horizon of 50 days as shown in Fig. 5.

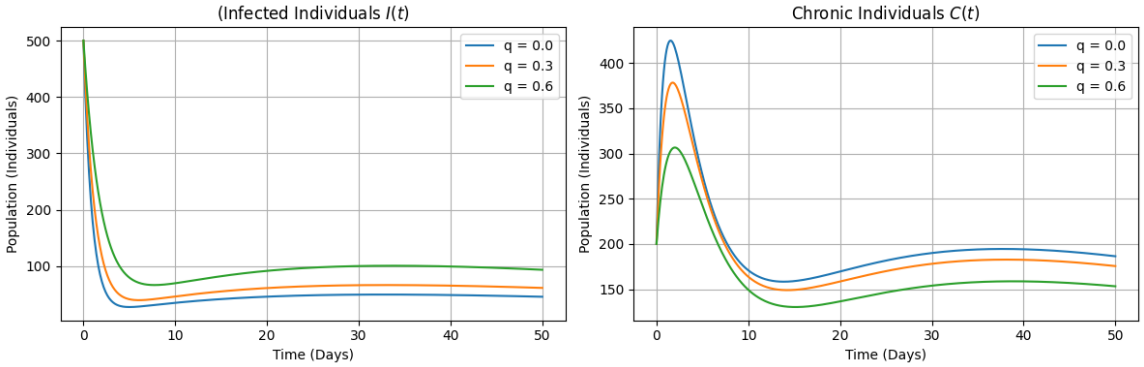

Fig. 5: Dynamic Population of the Infected and Chronic Compartment Under Different Individual Awareness Parameter Scenarios

The results demonstrate that variations in the parameter q have a notable impact on the dynamics of infected individuals $I(t)$ and chronic cases $C(t)$. For the infected compartment, all trajectories exhibit a rapid decline during the early phase, reflecting fast transitions within the system. However, higher values of q lead to a larger long-term level of infected individuals. Mathematically, this behavior suggests that the parameter q reduces the effective recovery rate or increases the persistence of individuals in the infected state.

3.5.6. Influence of Incidence Rate on Cardiovascular Complications

This subsection examines the role of the baseline incidence rate λ in shaping the dynamics of cardiovascular complications. Although the effective incidence is expressed as $\lambda(1-p)$, variations in λ represent differences in the underlying risk of developing the disease. The simulations show how changes in this rate influence both the number of affected individuals and the long-term accumulation of complications. From Table 2, the numerical simulation of dynamic model Eq. (1) with the inisial condition $I(0) = 500$, $C(0) = 200$, yields the time evolution of the compartments $I(t), C(t)$. The simulations are performed under three different scenarios of the parameter λ with $p = 0$ over a time horizon of 50 days as shown in Fig. 6.

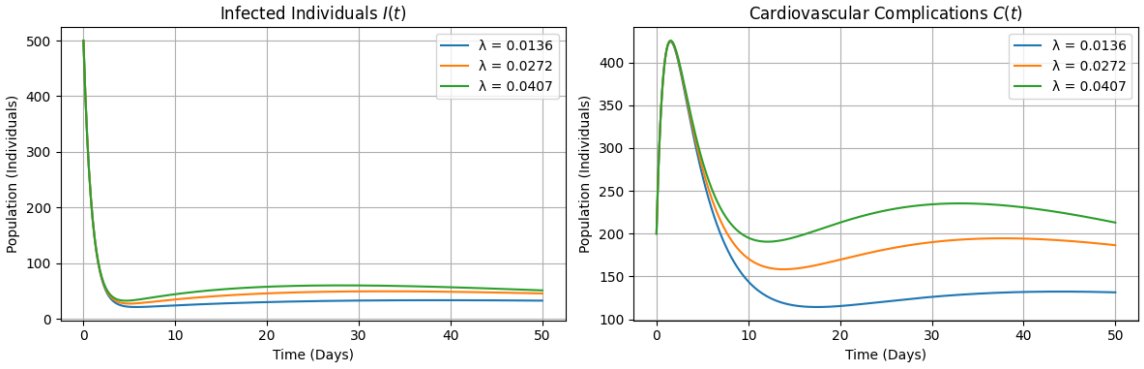

Fig. 6: Dynamic Population of the Infected and Chronic Compartment Under Different Baseline Incidence Rate Scenarios

The dynamics of the infected compartment $I(t)$ indicate that higher values of the baseline incidence rate λ lead to a more sustained level of affected individuals over the medium and long term, as the initial decline becomes slower due to increased inflow into the infected class, meanwhile, in the cardiovascular complication compartment $C(t)$, increasing λ produces higher peaks and elevated long-term levels, reflecting a greater accumulation of chronic cases, thus emphasizing that controlling the incidence rate is crucial to limit disease persistence and reduce the long-term burden of complications.

3.5.7. Effect of Disease Progression Rate on Complication Burden

This subsection examines the influence of the disease progression rate α on the evolution of affected individuals and the accumulation of cardiovascular complications. Although the progression term is expressed as $\alpha(1-q)$, parameters α and q represent fundamentally different mechanisms. The parameter α reflects the baseline clinical progression rate, while q captures behavioral modifications at the individual level. Therefore, analyzing variations in α provides insight into the intrinsic progression dynamics independent of awareness effects. From Table 2, the numerical simulation of dynamic model Eq. (1) with the inisial condition $I(0) = 500$, $C(0) = 200$, yields the time evolution of the compartments $I(t), C(t)$. The simulations are performed under three different scenarios of the parameter α with $q = 0$ over a time horizon of 50 days as shown in Fig. 7.

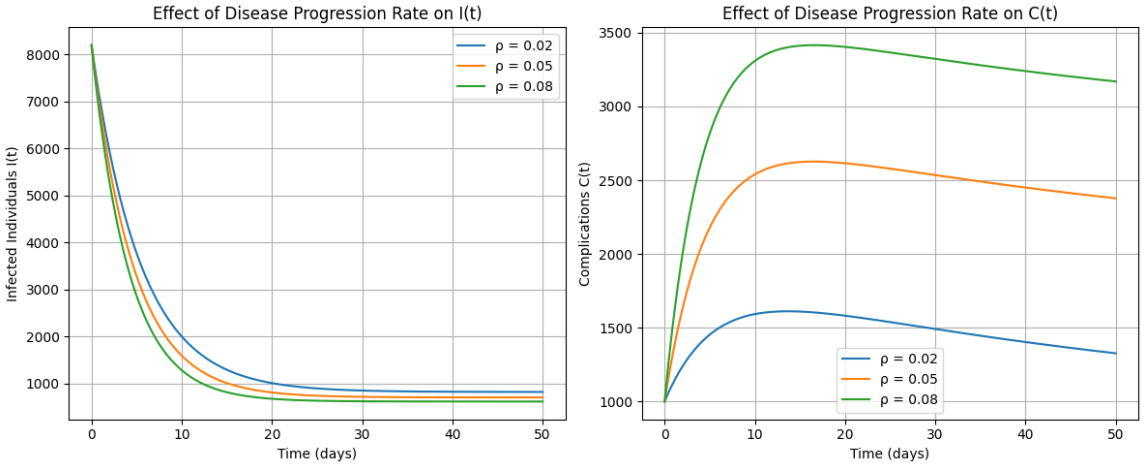

Fig. 7: Dynamic Population of the Infected and Chronic Compartment Under Different Disease Progression Rate Scenarios

The results show that increasing the disease progression rate α speeds up the decline in the infected population $I(t)$ by driving individuals more quickly to advanced stages, but at the same time leads to a higher and more persistent level in the complication compartment $C(t)$, indicating a greater accumulation of chronic cases; overall, this highlights a key trade-off in which faster early-stage reduction does not reduce the total disease burden, emphasizing that effective control strategies must also limit progression to chronic conditions, not just initial infection levels.

3.5.8. Two-Dimensional Analysis of Control Parameters on Chronic Disease Dynamics

This subsection presents a two dimensional numerical analysis to provide deeper insight into the combined influence of time and key control parameters on the dynamics of the chronic compartment $C(t)$. The analysis focuses on the roles of media awareness p, individual awareness q, baseline incidence rate λ, and disease progression rate α in shaping the temporal evolution of the chronic disease burden. Using the parameter values listed in Table 2, simulations of model Eq. (1) are conducted over a time horizon of 50 days and the inisial condition of chronic compartment is 200 individuals. The response of the chronic compartment $C(t)$ is evaluated under varying values of p, q, λ, and α, and the results are visualized as surface plots in Fig. 8.

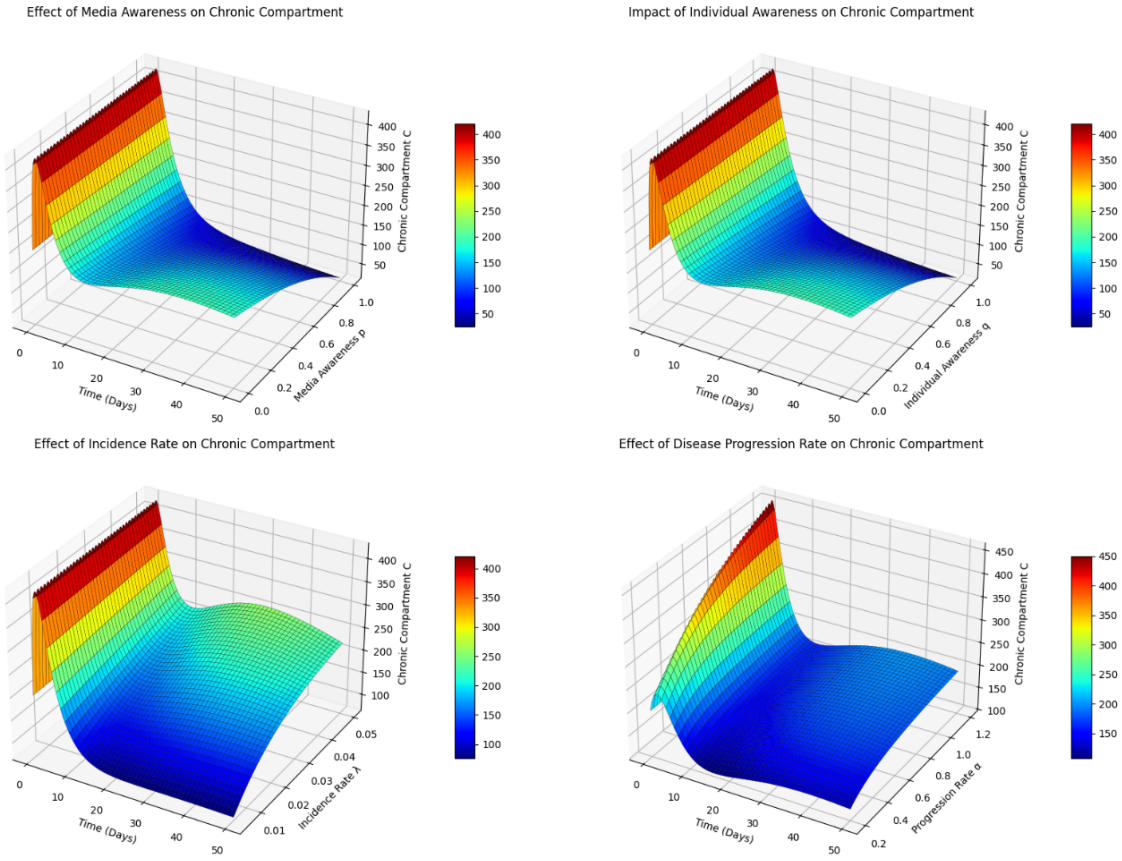

Fig. 8: Surface Plots of the Chronic Compartment Under Variations of Media Awareness p, Individual Awareness q, Baseline Incidence Rate λ, and Disease Progression Rate α

The three-dimensional results show that the chronic compartment $C(t)$ generally declines over time as it is shaped by the balance between inflow, recovery, and natural mortality, with higher media and individual awareness effectively reducing its magnitude by lowering the effective incidence rate; however, increasing the incidence and disease progression rates produces higher peaks and sustained long-term levels of $C(t)$, indicating that when transmission and progression dominate, they outweigh reduction effects, thus emphasizing the strong sensitivity of chronic disease dynamics to these key parameters.

4. Conclusion

This study develops and analyzes a compartmental model to explore the progression of cardiovascular disease under the influence of awareness-related and epidemiological factors. The numerical results demonstrate that both media awareness and individual awareness play a significant role in slowing disease progression by reducing the rate at which individuals move into higher-risk health states. As a result, the long-term burden of chronic complications is substantially decreased. These findings highlight the critical importance of awareness-based, non-pharmaceutical strategies in managing cardiovascular conditions.

In contrast, higher baseline incidence and faster progression rates markedly increase the accumulation of individuals in the chronic stage, even when the number of individuals in earlier stages declines more rapidly. The two-dimensional analysis further reveals inherent trade-offs within the system, indicating that improvements in early-stage conditions do not necessarily lead to a proportional reduction in long-term complications. This suggests that effective management strategies should not only focus on early detection but also on slowing disease progression. Overall, the proposed model provides a comprehensive framework for understanding the long-term dynamics of cardiovascular disease. It emphasizes the importance

of integrating awareness programs with strategies targeting disease progression, offering valuable insights for the development of sustainable prevention and intervention policies.

Credit Authorship Contribution Statement

Arista Fitri Diana: Conceptualization, Supervision, Project Administration, Funding Acquisition, Software, Writing-(Abstract, Numerical Simulation, and Conclusion), and Review. **Mia Siti Khumaeroh:** Methodology, Model Formulation, Stability Analysis, and Sensitivity Analysis. **Tarita Intan Soraya:** Introduction, Positivity Analysis, Boundaries Analysis, and References. **Agung Ginanjar:** Data Curation, Validation, Investigation, and Editing.

Declaration of Generative AI and AI-Assisted Technologies

During the preparation of this work, the authors used ChatGPT to enhance clarity, grammar, and readability. After using this tool, the authors reviewed and edited the content as needed and take full responsibility for the content of the publication.

Declaration of Competing Interest

The authors declare no competing interests.

Funding and Acknowledgments

This research is fully supported by the Research Grant of the Directorate of Research and Community Service, Ministry of Higher Education, Science, and Technology of the Republic of Indonesia under Contract Number 077/LL6/PL/AL.04/2025 and A.1/2/062010/LPPM/V/2025.

Data Availability

The data used in this study were obtained from secondary sources and clinical data provided by Roemani Muhammadiyah Hospital, Semarang. The secondary data are publicly available from relevant publications and official reports. The hospital data are not publicly available due to privacy and ethical restrictions but may be available from the corresponding author upon reasonable request and with permission from the hospital.

References

[1] O. R. Ojo, H. O. Francis, M. O. Awoleye, J. Chimezie, W. O. Agbonifo, and T. G. Adedeji. "A Scoping Review on Mathematical Modelling Techniques Used in Non-communicable Disease (NCD) Research". In: *Advances in Research* 26.3 (2025), pp. 437–458. DOI: 10.9734/air/2025/v26i31361.

[2] C. E. Agbo, R. T. Abah, and A. M. Abdullahi. "A Mathematical Modeling on the Stability Analysis of Heart Disease Dynamics". In: *Journal of Institutional Research, Big Data Analytics and Innovation* 1.1 (2024), pp. 195–202. https://fnasjournals.com/index.php/FNAS-JMNS/article/view/776/693.

[3] L. Ciumrnean et al. "Cardiovascular Risk Factors and Physical Activity for the Prevention of Cardiovascular Diseases in the Elderly". In: *International Journal of Environmental Research and Public Health* 19.1 (2022). DOI: 10.3390/ijerph19010207.

[4] D. Plass et al. "Estimating Risk Factor Attributable Burden: Challenges and Potential Solutions When Using the Comparative Risk Assessment Methodology". In: *Archives of Public Health* 80.1 (2022), pp. 1–12. DOI: 10.1186/s13690-022-00900-8.

[5] L. Jibril and O. Odetunde. "Mathematical Modeling and Optimal Control Analysis on Sedentary Behavior and Physical Activity in Relation to Cardiovascular Disease (CVD)". In: *Biomedical Statistics and Informatics* 5.4 (2020), p. 87. DOI: 10.11648/j.bsi.20200504.13.

[6] Cheffer. *Analysis of Cardiovascular Rhythms Using Mathematical Models*. PDF document. http://mecanon.coppe.ufrj.br/wp-content/uploads/2017/08/Heart-Cardiology_JCCM-21.pdf.

[7] D. Roy, O. Mazumder, A. Sinha, and S. Khandelwal. "Multimodal Cardiovascular Model for Hemodynamic Analysis: Simulation Study on Mitral Valve Disorders". In: *PLOS ONE* 16.3 (2021), pp. 1–28. DOI: 10.1371/journal.pone.0247921.

[8] A. Arzani and S. T. M. Dawson. "Data-Driven Cardiovascular Flow Modelling: Examples and Opportunities". In: *Journal of the Royal Society Interface* 18.175 (2021). DOI: 10.1098/rsif.2020.0802.

[9] S. G. Hafezi et al. *New Dynamic Approach Models to Estimate the Effect of Dietary Fatty Acids on Lipid Profiles and the Incidence of Cardiovascular Disease in the MASHAD Cohort Study*. Research Square. 2023. https://www.researchsquare.com/article/rs-3172809/v1.

[10] S. Lishak, G. Grigorian, S. V. George, N. C. Ovenden, R. J. Shipley, and S. Arridge. "A Variable Heart Rate Multi-Compartmental Coupled Model of the Cardiovascular and Respiratory Systems". In: *Journal of the Royal Society Interface* 20.207 (2023). DOI: 10.1098/rsif.2023.0339.

[11] N. W. Jannah, L. Aryati, and F. Adi-Kusumo. "A Mathematical Model of Social Interaction Between the Sufferers of Cardiovascular and Type 2 Diabetes Mellitus". In: *Communications in Biomathematical Sciences* 7.1 (2024), pp. 87–105. DOI: 10.5614/cbms.2024.7.1.5.

[12] J. M. Mutwiwa. "A Mathematical Model of Cardiovascular Disease Dynamics Incorporating Personal Risk Factors". In: *Asian Journal of Probability and Statistics* 27.6 (2025), pp. 74–83. DOI: 10.9734/ajpas/2025/v27i6768.

[13] M. Logambal, S. Padmasekaran, and S. Dickson. "Evaluation of the Stability of Heart Disease Mathematical Model: The Impact of Heart Attack and Chronic Heart Disease". In: *Proyecciones* 44.5 (2025), pp. 742–761. DOI: 10.22199/issn.0717-6279-6812.

[14] S. Y. Tee and A. A. M. Daud. "Mathematical Model and Analysis of Population Dynamics for Heart Failure and Heart Transplant". In: *Journal of Quality Measurement and Analysis* 21.1 (2025), pp. 69–85. DOI: 10.17576/jqma.2101.2025.04.

[15] A. F. Diana, T. I. Soraya, M. S. Khumaeroh, and M. I. Hajar. "Optimal Control of Cardiovascular Disease Using Pontryagin's Maximum Principle". In: *ZERO: Jurnal Sains, Matematika dan Terapan* 9.2 (2025), p. 443. DOI: 10.30829/zero.v9i2.25849.

[16] A. A. Zainuddin et al. "The Major Risk Factor of Stroke Across Indonesia; A Nationwide Geospatial Analysis of Universal Health Coverage Program". In: *Archives of Public Health* 83.1 (2025). DOI: 10.1186/s13690-025-01613-4.

[17] J. Y. Lee et al. "Long-Term Cardiovascular Events in Hypertensive Patients: Full Report of the Korean Hypertension Cohort". In: *Korean Journal of Internal Medicine* 38.1 (2023), pp. 56–67. DOI: 10.3904/kjim.2022.249.

[18] World Health Organization. *World Health Statistics 2025*. 2025. https://www.who.int/publications/b/78420.

[19] E. S. Darmawan, S. R. Hasibuan, V. Y. Permanasari, and D. Kusuma. "Disparities in Cancer Care and Outcomes by Insurance Membership Type in Indonesia: A Retrospective Cross-Sectional Analysis of National Health Insurance Claims, 2017–2022". In: *BMJ Open* 15.7 (2025). DOI: 10.1136/bmjopen-2024-096486.

[20] F. R. Muharram et al. "The 30 Years of Shifting in The Indonesian Cardiovascular Burden—Analysis of The Global Burden of Disease Study". In: *Journal of Epidemiology and Global Health* 14.1 (2024), pp. 193–212. DOI: 10.1007/s44197-024-00187-8.

[21] B. Dwiputra et al. "Risk Estimation for Recurrent Cardiovascular Events Using the SMART-REACH Model and Direct Inpatient Cost Profiling in Indonesian ASCVD Patients: A Large-Scale Multicenter Study". In: *Frontiers in Cardiovascular Medicine* 11.August (2024), pp. 1–9. DOI: 10.3389/fcvm.2024.1425703.

[22] W. Frk, A. Wojtasiska, W. Lisiska, E. Mynarska, B. Franczyk, and J. Rysz. "Pathophysiology of Cardiovascular Diseases: New Insights into Molecular Mechanisms of Atherosclerosis, Arterial Hypertension, and Coronary Artery Disease". In: *Biomedicines* 10.8 (2022). DOI: 10.3390/biomedicines10081938.

[23] World Health Organization. *World Health Statistics 2019*. Bibliographic data in the source list is incomplete. 2019. file:///Users/macbook/Downloads/547-Article%20Text-2022-1-10-20200417.pd.

[24] Badan Pusat Statistik. *Badan Pusat Statistik Provinsi Jawa Tengah Dalam Angka 2020*. Vol. 3, No. 2, p. 861. 2020. https://bit.ly/4tYFHnB.

[25] Pemerintah Provinsi Jawa Tengah. *Laporan Demografi Jawa Tengah Tahun 2021*. 2021. https://bit.ly/4wPzY6b.

[26] Adhi Wiriana. *Laporan Demografi Jawa Tengah Tahun 2022*. 2022. https://jateng.bps.go.id/id/publication/2022/02/25/431f4f4bbe02b47866b357cc/provinsi-jawa-tengah-dalam-angka-2022.html.

[27] Dinas Pemberdayaan Masyarakat dan Provinsi Jawa Tengah. *Laporan Demografi Jawa Tengah Tahun 2023*. 2023. https://bit.ly/4dyEVZy.

[28] Dinas Kesehatan Jawa Tengah. *Laporan Demografi Jawa Tengah Tahun 2024*. Profil Kesehatan Provinsi Jawa Tengah Tahun 2024, Vol. 3, pp. 1–260. 2024. https://bit.ly/4dBJvVy.

[29] E. Astutik, S. I. Puspikawati, D. M. S. K. Dewi, A. M. Mandagi, and S. K. Sebayang. "Prevalence and Risk Factors of High Blood Pressure Among Adults in Banyuwangi Coastal Communities, Indonesia". In: *Ethiopian Journal of Health Sciences* 30.6 (2020), pp. 941–950. DOI: 10.4314/ejhs.v30i6.12.

[30] Food Technology. "Coronary artery disease incidence, risk factors, awareness, and medication utilization in a 10- year cohort study". In: *BMC Cardiovascular Disorders* 24.101 (2024). https://doi.org/10.1186/s12872-024-03769-3.